OPEN ACCESS

Original research

Mass cytometry-based peripheral blood analysis as a novel tool for early detection of solid tumours: a multicentre study

Qi Zhang ,[1,2,3,4,5,6] Mao Ye,[1,2] Cheng Lin,[7] Manyi Hu,[1] Yangyang Wang,[1] Yu Lou,[1,2] Quanming Kong,[7] Jungang Zhang,[8] Junjian Li,[9] Yuhua Zhang,[10] Tianxing Yang,[11] Xu Sun,[12] Weiyun Yao,[13] Yongfei Hua,[14] Haifeng Huang,[15] Minghui Xu,[16] Xiaoguang Wang,[17] Xin Yu,[18] Weifeng Tao,[19] Runtian Liu,[20] Yuming Gao,[21] Tian Wang,[7] Jianing Wang,[1,2] Xiaobao Wei,[1,2] Jiangchao Wu,[1,2] Zhengping Yu,[9] Chengwu Zhang,[8] Chaohui Yu ,[22] Xueli Bai ,[1,2,3,4,5] Tingbo Liang[1,2,3,4,5]

► Additional supplemental material is published online only. To view, please visit the journal online (http://dx.doi.org/10.1136/gutjnl-2022-327496).

For numbered affiliations see end of article.

Correspondence to
Professor Tingbo Liang, Department of Hepatobiliary and Pancreatic Surgery, the First Affiliated Hospital, Zhejiang University School of Medicine, No. 79 Qingchun Road, Hangzhou 310003, China; liangtingbo@zju.edu.cn

QZ, MY and CL contributed equally.

Received 31 March 2022
Accepted 8 September 2022
Published Online First 16 September 2022

To cite: Zhang Q, Ye M, Lin C, *et al*. *Gut* 2023;**72**:996–1006.

ABSTRACT

Objective Early detection of a tumour remains an unmet medical need, and approaches with high sensitivity and specificity are urgently required. Mass cytometry time-of-flight (CyTOF) is a powerful technique to profile immune cells and could be applied to tumour detection. We attempted to establish diagnostic models for hepatocellular carcinoma (HCC) and pancreatic ductal adenocarcinoma (PDAC).

Design We performed CyTOF analysis for 2348 participants from 15 centres, including 1131 participants with hepatic diseases, 584 participants with pancreatic diseases and 633 healthy volunteers. Diagnostic models were constructed through random forest algorithm and validated in subgroups.

Results We determined the disturbance of systemic immunity caused by HCC and PDAC, and calculated a peripheral blood immune score (PBIScore) based on the constructed model. The PBIScore exhibited good performance in detecting HCC and PDAC, with both sensitivity and specificity being around 80% in the validation cohorts. We further established an integrated PBIScore (iPBIScore) by combining PBIScore and alpha-fetoprotein or carbohydrate antigen 19-9. The iPBIScore for HCC had an area under the curve (AUC) of 0.99, 0.97 and 0.96 in training, internal validation and external validation cohorts, respectively. Similarly, the iPBIScore for PDAC showed an AUC of 0.99, 0.98 and 0.97 in the training, internal validation and external validation cohorts, respectively. In early-stage and tumour-marker-negative patients, our iPBIScore-based models also showed an AUC of 0.95–0.96 and 0.81–0.92, respectively.

Conclusion Our study proved that the alterations of peripheral immune cell subsets could assist tumour detection, and provide a ready-to-use detection model for HCC and PDAC.

WHAT IS ALREADY KNOWN ON THIS TOPIC

⇒ Early detection of cancer helps patients receive timely treatment and improves their prognosis.
⇒ Tumour-burdened mouse models demonstrated the relationship between existence of tumour and systemic dysfunction of the immune macroenvironment.
⇒ Cytometry time-of flight (CyTOF) as a novel technology, could profile the composition and number of immune cells, reflecting immunity in higher-dimensional plane.

WHAT THIS STUDY ADDS

⇒ Our study determined the alterations of peripheral immune cell subsets caused by hepatocellular carcinoma (HCC) or pancreatic ductal adenocarcinoma (PDAC) in humans through CyTOF analysis for peripheral blood.
⇒ Constructed models based on selected cell markers and subsets that obtained from CyTOF and random forest algorithm exhibited excellent performance in detecting patients with malignancies.

HOW THIS STUDY MIGHT AFFECT RESEARCH, PRACTICE OR POLICY

⇒ CyTOF serves as potential tool that assist in detection of HCC and PDAC, which also indicated that CyTOF may develop as novel tool method used in multicancer screening for its higher dimension of description for system immune.

INTRODUCTION

Malignant tumours, such as hepatocellular carcinoma (HCC) and pancreatic ductal adenocarcinoma (PDAC), are characterised by insidious onset, leading to a delay in diagnosis and treatment. Routine serological tests currently used in the clinic are limited by their low sensitivity or low specificity. For instance, alpha-fetoprotein (AFP) has a sensitivity of less than 50%, and acute liver disease and pregnancy are often accompanied by elevated AFP.[1–3] Similarly, approximately 20% of patients with PDAC are negative for carcinoma antigen 19-9 (CA19-9),[4] while benign obstruction of the bile

duct and impaired renal function frequently cause an increased level of CA19-9.[5–7] Thus, novel tools for tumour screening and early-stage detection are urgently needed.

The emerging technique of liquid biopsy, which is mainly related to detection of circulating tumour DNA (ctDNA), cell-free RNAs (eg, messenger RNAs, microRNAs), circulating tumour cells (CTCs) and exosomes,[8] attempts to replace traditional serological screening methods or tissue biopsy. In HCC, for example, a serum metabolic panel, 5-hydroxymethylcytosines and ctDNA, exhibited good performance in detection of HCC in patients, with an area under the curve (AUC) ranging from 0.8 to 0.9.[9–11] These strategies have demonstrated their strengths and potential in the field of tumour detection. However, there are currently no well-accepted liquid biopsy strategies for tumour detection.

Over the past decade, the development of immunotherapy has changed the decision-making of cancer treatment, with success in many types of cancer.[12–14] The rapid development of immunotherapy has deepened our understanding of the relationship between cancer and the immune system. A recent study using mouse models discovered tumour-induced systemic dysfunction of the immune macroenvironment, which could be restored by tumour resection.[15] In addition, individual immunity is coordinated across tissues, and the local antitumour immune response depends on continuous communication with the peripheral blood.[16 17] For example, a considerable proportion of regulatory T cells (Tregs) within tumours are derived from naturally occurring thymic Tregs.[18] The frequency and status of immune cells change dynamically during tumour progression.[15] Moreover, the number of regulatory B cells increased in the peripheral blood of patients with gastric cancer and lung cancer, and the expression of the inhibitory receptor of natural killer (NK) cells increased in the peripheral blood of patients with breast cancer.[19–21] Increasing evidence supports the view that the occurrence and development of tumours are accompanied by systemic immune disturbance and alternations of peripheral immune cells.[15 22–24] Therefore, immune profiling of the circulation might help to detect tumours; however, no such successful attempt has been made to date.

Mass cytometry by time-of-flight (CyTOF) is a newly developed technology that can profile the composition and number of immune cells.[25–27] To test the value of peripheral blood immune cells in tumour detection, we launched a large-volume, multicentre study and used CyTOF to obtain the comprehensive information of immune cell composition, phenotype and function in peripheral blood. The aim of this study was to establish diagnostic models for HCC and PDAC using CyTOF, and to try to understand the logic underlying the models for their better clinical application.

MATERIALS AND METHODS

Participant cohorts

This was a multicentre, prospective study that recruited a total of 2348 participants from 15 centres across China from October 2019 to July 2022. The training cohort and internal validation cohort were from the leading centre (The First Affiliated Hospital, Zhejiang University School of Medicine). Using an age-stratified random sampling method, we selected 900 and 500 of them to construct the training cohort of hepatic group and pancreatic group, respectively. The remaining participants from the leading centre were used for internal validation. The external validation cohort included participants from the other 14 centres in four provinces (online supplemental table S1). For the internal and external validation cohorts, all participants' information and diagnoses were blinded for the experimenters and analysers. Diagnoses of the included participants were confirmed using ultrasound, CT or MRI. In particular, HCC was determined by pathology or clinical diagnosis, and PDAC was determined by pathology according to clinical guidelines. The diagnosis of patients who received surgical resection was further confirmed by histopathology. Hepatic benign diseases included, but were not limited to, haemangiomas (164 cases), cysts (66 cases) and focal nodular hyperplasia (71 cases). Pancreatic benign diseases included, but were not limited to, neuroendocrine tumours (28 cases), cystic neoplasms (120 cases), autoimmune pancreatitis (9 cases) and chronic pancreatitis (18 cases). Peripheral blood samples from the healthy volunteers were collected during routine physical examination. Their health statuses were determined by reviewing medical examination results and consulting medical history. The exclusion criteria were as follows: A history of cancer-related treatment; acute infections; blood transfusion within the past 6 months; use of drugs affecting the composition of peripheral blood, such as recombinant human erythropoietin and interleukins, within the past 2 weeks; recurrent tumours; decompensated dysfunction of organs; immune deficiency syndrome; haematological precancerous diseases; receiving immunosuppressive therapy; and confirmed coagulopathy.

Sample collection and processing

Peripheral blood sample (5 mL per person) of each participant was collected before any antitumour treatments. The collected samples were transported to the laboratory for processing within 12 hours at room temperature or within 48 hours at about 4°C. All samples had not been cryopreserved and all analysis was performed on fresh samples of blood. Peripheral blood mononuclear cells (PBMCs) were isolated from the peripheral blood by density gradient centrifugation using Ficoll. The cell precipitates were resuspended in 5 mL of pre-cooled fluorescence activated cell sorting (FACS) buffer (1×phosphate buffered saline (PBS) supplemented with 0.5% bovine serum albumin), and then centrifuged at 400×*g* for 5 min at 4°C. The supernatant was discarded and the cell precipitates were resuspended in FACS buffer again. The number of cells was counted and the quality of samples for subsequent analysis should meet the following requirement: The number of cells should not be less than 3×10^6 and the viability rate should be higher than 85%.

CyTOF staining and data acquisition

The provider, clone number and mass tag of each antibody used in this study are showed in online supplemental table S2. Antibody labelling with mass tag was performed using the Maxpar antibody conjugation kit (Fluidigm). The concentration of mass-tagged antibody was assessed by NanoDrop. Antibody stabiliser buffer was used to adjust the concentration of labelled antibody to 200 mg/mL. Titration of conjugated antibodies should be performed to get optimal concentration for use. Obtained cells were washed with PBS, stained with 100 µL of 250 nM cisplatin (Fluidigm, South San Francisco, California, USA) for 5 min on ice to exclude dead cells and incubated in Fc receptor blocking solution before being stained with a surface antibodies cocktail for 30 min on ice. After washed with PBS, we use unique barcoding isotope combination to label individual cell samples for 30 min. Cells were washed twice with FACS buffer and fixed in 200 µL of intercalation solution (Maxpar Fix and Perm Buffer containing 250 nM 191/193Ir, Fluidigm) overnight. After fixation, the cells were washed with FACS buffer and then with Perm Buffer (eBioscience, San Diego, California, USA), and stained

with an intracellular antibodies cocktail for 30 min on ice. Cells were washed and resuspended in deionised water, added into 20% EQ beads (Fluidigm) and applied to a mass cytometer (Helios, Fluidigm). The CyTOF experiments were performed by PLTTECH (Hangzhou, China). Before each batch of samples were loaded, the instrument adjusted the signal strength of each channel according to the same beads signal (140Ce,151Eu,153Eu,165Ho,175Lu). All samples were standardised to avoid batch effect before analysis.

CyTOF data analysis

Data for each sample were de-barcoded from the raw data using a doublet-filtering scheme with unique mass-tagged barcodes.[28] Each .fcs file generated from different batches were normalised using the bead normalisation method.[29] We used the FlowJo software (FlowJo, Ashland, Oregon, USA) to exclude to debris, dead cells and doublets from the manual gating data, leaving only live single immune cells. We applied the X-shift clustering algorithm to all cells to partition the cells into distinct phenotypes based on marker expression levels,[30] and then annotated the cell type of each cluster according to its marker expression pattern on a heatmap of clusters and markers. The dimensionality reduction algorithm, t-distributed stochastic neighbour embedding, was used to visualise the high-dimensional data in two dimensions, to show the distribution of each cluster and marker expression and the difference among the groups or different sample types.[31] Student's t-test statistical analysis was performed on the frequency of annotated cell populations.

Model construction

The data set was divided into three parts: training set, internal validation set and external validation set. Marker negative proportion and subgroup proportion were used as modelling features. Due to the excessive number of features, there may be some collinearity and non-significant features, so it is necessary to conduct feature screening to screen out important and useful features. The training set and internal validation set were then used to select features. The models were constructed using a random forest algorithm. In brief, features were selected according to their highest score, and 300 samples were selected randomly from negative and positive samples, respectively, to establish a random forest model. A 10-fold cross-validation method was adopted to obtain the average importance of each feature. If this process was repeated 1000 times, each feature would have 1000 feature importance values. We counted the number of features whose importance was greater than 0.01 for each feature. If the number was greater than 400, the feature was selected. Subsequently, the selected features were used as required features for modelling. Based on the screened features, the random forest model was constructed again after standardised processing of the training set, and the 10-fold cross-validation method was adopted to make each sample participate in modelling and testing, so as to eliminate the influence of sample differences on the model and find the optimal hyperparameter of the model. Then, the generalisation abilities of the constructed models were evaluated in internal validation set and external validation set, to further prove the robustness of the models. The peripheral blood immune score (PBIScore) of each participant was obtained from the models. For instance, a new sample was put into the well-trained model, and the probability of this sample belonging to malignancy was judged by each decision tree in the random forest model. The average probability obtained by all decision trees was recorded as the PBIScore of this sample, ranging from 0 to 1. We discretised the data of AFP and CA19-9. In the hepatic group, if the AFP level was higher than 20 ng/mL (the upper limit of normal level), the value was assigned to 0; otherwise, the value was assigned to 1. We set the normal upper limit of CA19-9 at 37 U/mL and performed a similar assignment strategy. The discrete index was added to the corresponding model as a feature, and the random forest model was established again. Similarly, the score of the new sample was calculated as above method according to the new random forest model, which was denoted as integrated peripheral blood immune score (iPBIScore).

Statistical analysis

The data are presented as the mean±SD or SEM. Student's t-test, the Wilcoxon rank-sum test, or the Z test were used for statistical analysis, as appropriate. Data analysis was performed using the SPSS software (V.24; IBM, Armonk, New York, USA). A p value <0.05 was considered statistically significant.

RESULTS

Baseline characteristics of cohorts

A total of 2348 participants were included in this study, including 1131 patients with hepatic diseases, 584 patients with pancreatic diseases and 633 healthy volunteers as controls. The hepatic group was consisted of 790 patients with HCC and 341 patients with benign hepatic diseases. The pancreatic group included 376 patients with PDAC and 208 patients with benign pancreatic diseases. Healthy controls were shared by both groups. The demographic and clinicopathological characteristics of all participants are presented in online supplemental tables S3–S6.

Tumours are associated with altered peripheral immune cell subsets

The phenomenon of increased proliferation of immature neutrophils and monocytes in tumour-bearing models has been widely reviewed in previous studies,[32 33] which indicated that changes of peripheral immune cells may reflect the existence of insidious tumours. Therefore, we speculated that similar disturbances of systemic immunity existed in patients with HCC or PDAC, which could serve as novel tumour screening markers. To reveal the profiles of peripheral immunity, we performed the CyTOF analysis to all collected PBMC samples. All CyTOF data were pre-processed and living single immune cells ($CD45^+$) were retained after gating for further analysis. To exhibit the expression of different markers in various immune cells, but limited to the excessively large number of cells, we randomly selected cases from each group including 81 cases of HCC, 50 cases of benign hepatic diseases, 50 cases of PDAC, 50 cases of benign pancreatic diseases and 50 healthy volunteers. We then drew heatmap based on their CyTOF analysis results. Based on the canonical cell surface markers, we defined 32 major cell clusters, including 9 clusters of $CD4^+$ T cells ($CD3^+CD4^+$), 8 clusters of $CD8^+$ T cells ($CD3^+CD8^+$), 3 clusters of B cells ($CD3^-CD19^+$), 2 clusters of monocytes ($CD3^-CD19^-CD14^+$) and 10 clusters of other subsets, such as dendritic cells (DCs, $CD3^-CD19^-CD14^-CD20^-HLA\text{-}DR^+$), and NK cells ($CD3^-CD19^-CD14^-CD20^-CD56^+$) (figure 1A,B).

We then analysed the differences in participants with or without malignant tumours in the hepatic group and pancreatic group, respectively, and found significant differences for some cell subsets in both scenarios (figure 1C). Compared with the participants without malignancies (named 'non-HCC', including healthy volunteers and cohort with hepatic benign

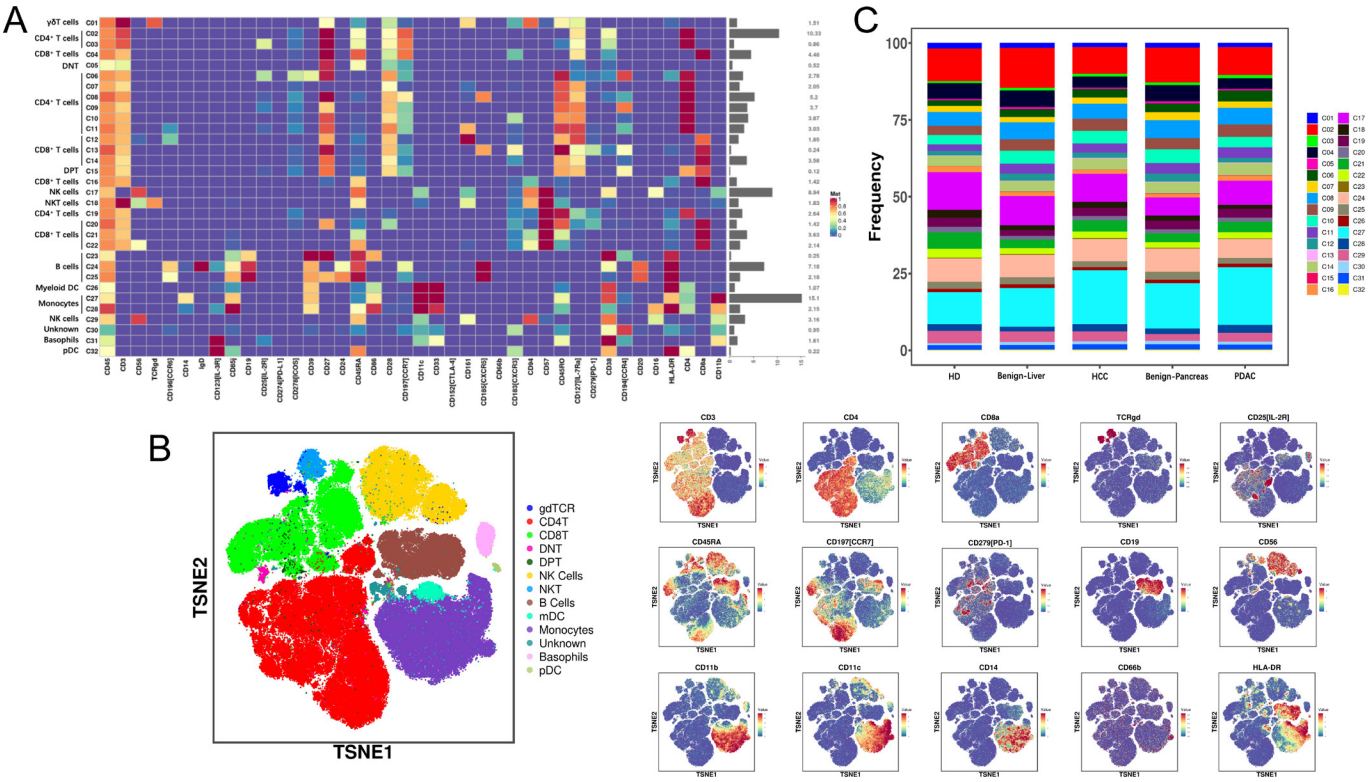

Figure 1 Profile of peripheral immune status. The CyTOF data from randomly selected cases that are representative of each cohort (including 81 HCC, 50 liver benign diseases, 50 pancreatic cancer, 50 pancreatic benign diseases and 50 healthy people) are shown. (A) Heatmap of normalised expression for markers expressed in peripheral immune cells. Types and proportions of various immune cells are presented in left and right of heatmap, respectively. (B) Visualised t-SNE map of definition of peripheral immune cells from CyTOF data of 281 selected cases and part selected classical cell surface markers used for annotation of various immune cells. (C) Frequency diagram of immune cell subsets in the different groups. Benign-liver, hepatic benign diseases; Benign-pancreas, pancreatic benign diseases; CyTOF, cytometry time-of-flight; DNT, double negative T cells; DPT, double positive T cells; double positive T cells; HD, healthy donor; HCC, hepatocellular carcinoma; mDC, myeloid dendritic cells; NK, natural killer; PDAC, pancreatic ductal adenocarcinoma; gdTCR: γδ T cells; pDC, plasmacytoid dendritic cells; t-SNE, t-distributed stochastic neighbour embedding.

diseases), participants with HCC presented with decreased levels of naïve $CD4^+$ T cells (C02, $CD4^+CCR7^+CD45RA^+$), naïve $CD8^+$ T cells (C04, $CD8^+CCR7^+CD45RA^+$), effector $CD8^+$ T cells (C16, $CD8^+CCR7^-CD45RA^+$) and memory B cells (C25, $CD19^+CD27^+$), while the levels of $CD39^+$ naïve $CD4^+$ T cells (C06, $CD4^+CCR7^+CD45RA^+CD39^+$), central memory $CD4^+$ T cells (C09, $CD4^+CCR7^+CD45RA^-$), double positive T cells (C15, $CD4^+CD8^+$), plasma cells (C23, $CD19^+CD27^+CD20^-CD38^+$) and monocytes (C27 and C28, $CD3^-CD19^-CD14^+$) were increased (online supplemental figure S1). Intriguingly, some subsets showed an aggravation-related change from early-stage to late-stage tumours (online supplemental figure S2). For instance, the increasement of NK cells (C17) was more significant in HCC from stage 0 to stage C, while a subset of $CCR4^+CD20^-$ B cells (C23) gradually reduced as the Barcelona Clinic Liver Cancer stage advanced.

A similar phenomenon was observed in the pancreatic group. Compared with participants without PDAC (include healthy volunteers and cohort with pancreatic benign diseases), lower levels of naïve $CD4^+$ T cells (C02, $CD4^+CCR7^+CD45RA^+$), naïve $CD8^+$ T cells (C04, $CD8^+CCR7^+CD45RA^+$), naïve B cells (C24, $CD19^+CD27^-$) and memory B cells (C25, $CD19^+CD20^+CD27^+$) were observed in patients with PDACs, while the levels of central memory $CD4^+$ T cells (C03, $CD4^+CCR7^-CD45RA^+$), plasmacytoid DCs (C32, $CD3^-CD19^-CD14^-CD20^-HLA\text{-}DR^+CD123^+$) and monocytes (C27 and C28, $CD3^-CD19^-CD14^+$) were higher (online supplemental figure S3). Analysis of cell subsets between different stages of PDAC was also performed (online supplemental figure S4). The frequency of C03 subset increased as the stage of PDAC advanced, and that of C12 and C13 subsets gradually decreased with the stage of PDAC advanced. These results indicated that tumour-bearing hosts did have altered immune cell subsets in the periphery, which might be used to screen for malignancies.

Potential markers and immune cell subsets for model construction

For the HCC diagnostic model, the training cohort contained 450 participants with HCC, 150 participants with benign hepatic diseases and 300 healthy controls. The remaining 199 patients with HCC and 71 participants with hepatic diseases as well as 302 healthy controls from the leading centre were defined as the internal validation cohort to verify the efficacy of the model. Another 141 patients with HCC, 120 participants with benign hepatic diseases and 31 healthy volunteers from the 14 cooperating centres comprised the external validation cohort, which was used to confirm the generalisation ability of the models (figure 2). Participants in the pancreatic group were similarly grouped to construct and validate the diagnostic model for PDAC.

Provided that participants with malignancies had distinct immune profiles in their circulation, we first tried to identify potential parameters (eg, markers or immune cell subsets) for

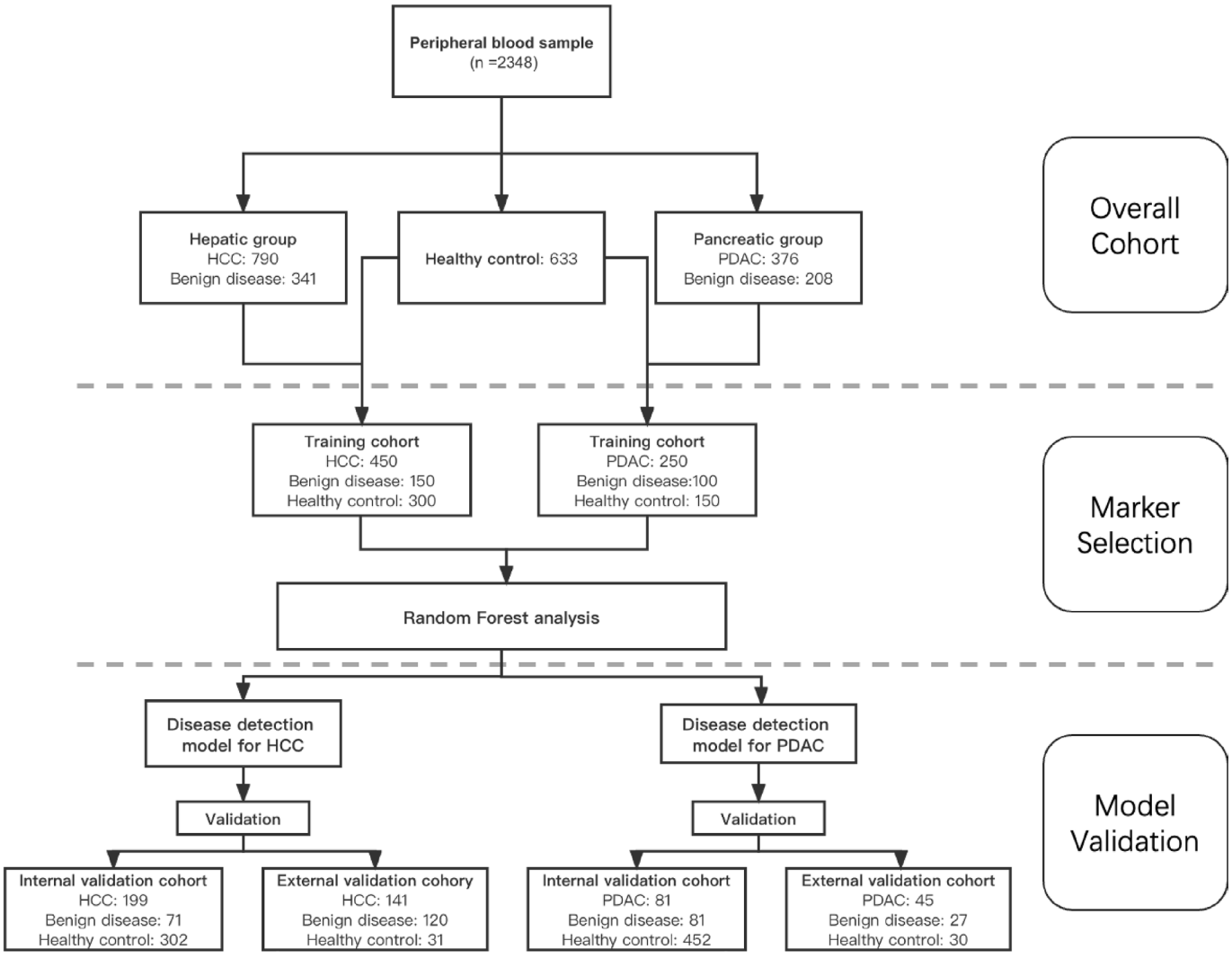

Figure 2 Workflow chart. A total of 2348 peripheral blood samples were collected prospectively from 15 centres. Healthy controls and patients with benign diseases were assigned as the non-malignant group. Marker selection was performed based on the differences between participants with or without malignancies. Healthy controls were shared with the hepatic and pancreatic groups. Random forest analysis was used to generate detection models for HCC and PDAC, respectively. The models were validated using internal and external validation cohorts. HCC, hepatocellular carcinoma; PDAC, pancreatic ductal adenocarcinoma.

tumour detection. We employed the well-established random forest algorithm to discover consequential features from the training groups of HCC and PDAC, respectively. In the hepatic group, we determined 7 markers and 16 cell subsets with the potential to discriminate HCC from non-HCC participants (online supplemental table S7). In the pancreatic group, we obtained 8 markers and 11 cell subsets for PDAC screening (online supplemental table S8). These cell subsets contained monocytes, B cells and T cells. These markers and cell subsets were then applied to construct diagnostic models.

Diagnostic and differentially diagnostic efficacies of the models based on PBIScore

In the training cohort of the hepatic group, the PBIScore of the participants with HCC was significantly higher than that of the non-HCC subjects (0.753 vs 0.247; figure 3A). Similar results were observed in the internal validation and external validation cohorts. This diagnostic model based on the PBIScore alone achieved a sensitivity of 90.2% and a specificity of 92.0%, with an area under the receiver-operating characteristic curve of 0.98 (figure 3B). In the internal validation cohort, the sensitivity was 80.9% and the specificity was 86.9% (AUC=0.91), and in the external validation cohort, the sensitivity and specificity reached 83.0% and 78.2%, respectively. We then combined the AFP level and PBIScore together (named as iPBIScore) to generate a new model, which had a higher sensitivity of 93.1% and specificity of 98.7% in the same training cohort, with an AUC of 0.99. Similarly, the sensitivity and specificity in the two validation cohorts were further improved compared with the PBIScore alone. The AUC values of the iPBIScore in the internal validation cohort and external validation cohort were 0.97 and 0.96, respectively, which were superior to that of AFP alone (AUC, 0.84–0.83).

To test our strategy in pancreatic cancer, we performed a similar study. The PBIScore was significantly higher in participants with PDAC than in non-PDAC participants for all cohorts tested (figure 4A). The model using the PBIScore alone for PDAC screening achieved a sensitivity of 92.4% and specificity of 91.2%, with an AUC of 0.98 in the training cohort (figure 4B). Our model also showed a good discrimination ability in both the internal validation cohort (AUC=0.89) and

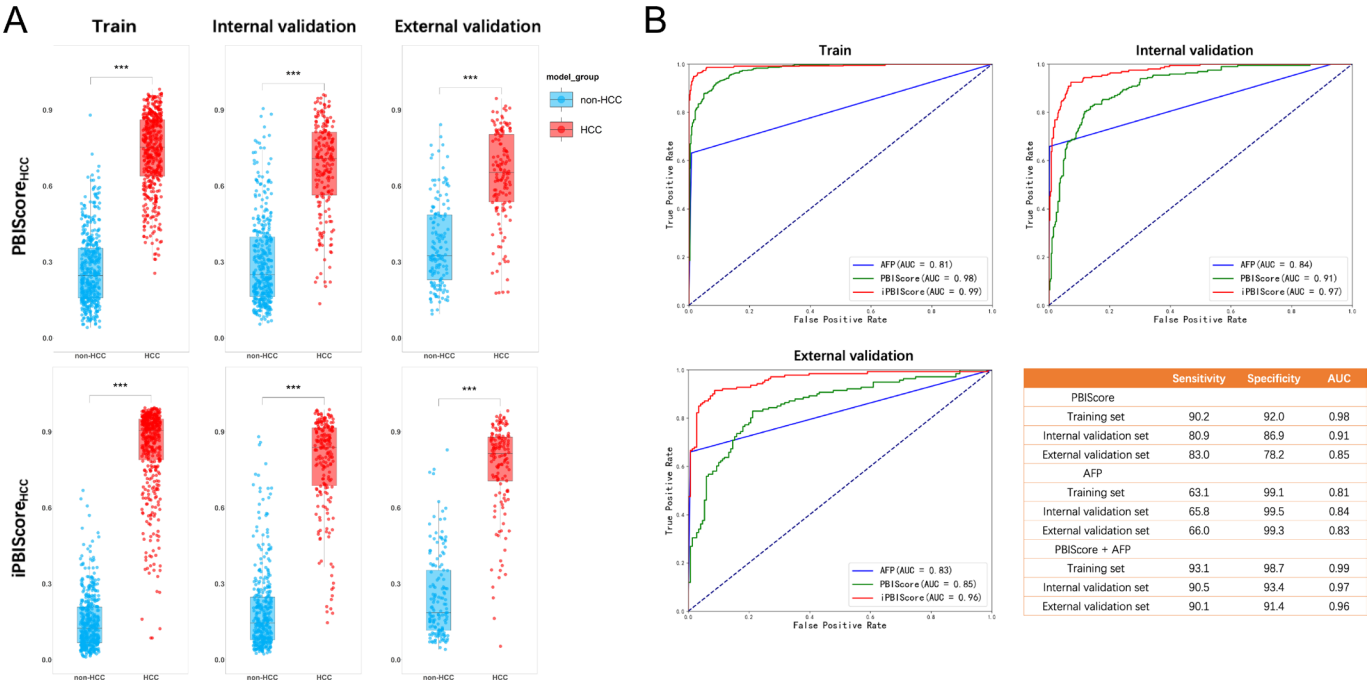

	Sensitivity	Specificity	AUC
PBIScore			
Training set	90.2	92.0	0.98
Internal validation set	80.9	86.9	0.91
External validation set	83.0	78.2	0.85
AFP			
Training set	63.1	99.1	0.81
Internal validation set	65.8	99.5	0.84
External validation set	66.0	99.3	0.83
PBIScore + AFP			
Training set	93.1	98.7	0.99
Internal validation set	90.5	93.4	0.97
External validation set	90.1	91.4	0.96

Figure 3 Development and validation of the HCC detection models. (A) The PBIScore and iPBIScore of participants with or without HCC in the training cohort, internal validation cohort and external validation cohort. (B) The ROC curves of AFP, PBIScore and iPBIScore for HCC detection in the training cohort, internal validation cohort and external validation cohort. Table showing the sensitivity, specificity and AUC value of the three strategies for HCC in different cohorts. ***, p< 0.001. AFP, alpha-fetoprotein; AUC, area under the curve; HCC, hepatocellular carcinoma; iPBIScore, integrated peripheral blood immune score; PBIScore, peripheral blood immune score; ROC, receiver operating characteristic.

the external validation cohort (AUC=0.89). While CA19-9, the most frequently used tumour marker in clinical practice, showed an AUC of 0.92−0.86, the combined model of PBIScore and CA19-9 had AUC values of 0.99, 0.98 and 0.97 in the training cohort, internal validation cohort and external validation cohort, respectively.

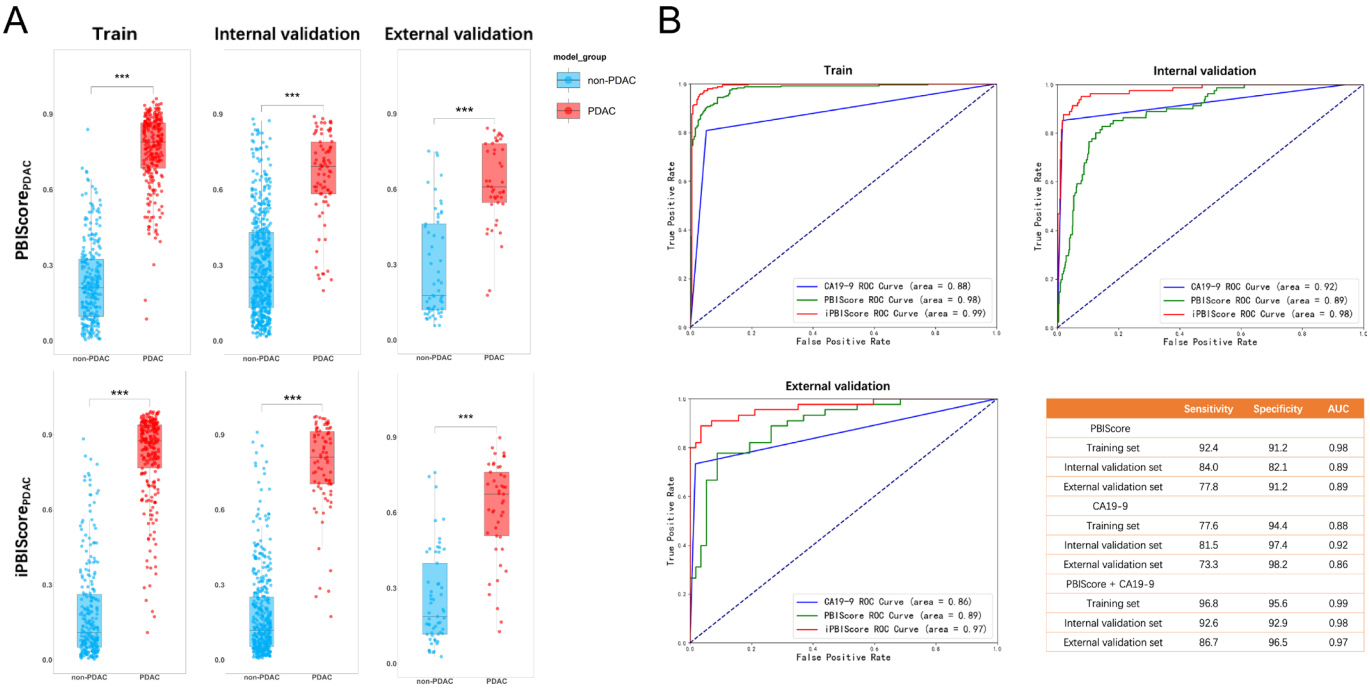

	Sensitivity	Specificity	AUC
PBIScore			
Training set	92.4	91.2	0.98
Internal validation set	84.0	82.1	0.89
External validation set	77.8	91.2	0.89
CA19-9			
Training set	77.6	94.4	0.88
Internal validation set	81.5	97.4	0.92
External validation set	73.3	98.2	0.86
PBIScore + CA19-9			
Training set	96.8	95.6	0.99
Internal validation set	92.6	92.9	0.98
External validation set	86.7	96.5	0.97

Figure 4 Development and validation of PDAC detection models. (A) The PBIScores and iPBIScore of participants with or without PDAC in the training cohort, internal validation cohort and external validation cohort. (B) The ROC curves of CA19-9, PBIScore and iPBIScore for PDAC detection in the training cohort, internal validation cohort and external validation cohort. Table showing the sensitivity, specificity and AUC value of the three strategies for PDAC in different cohorts. ***, P< 0.0001. AUC, area under the curve; CA19-9, carcinoma antigen 19-9; iPBIScore, integrated peripheral blood immune score; PBIScore, peripheral blood immune score; PDAC, pancreatic ductal adenocarcinoma; ROC, receiver operating characteristic.

Although the original aim of our study is to develop a tool for tumour diagnosis, we wondered the efficacy of our PBIScore-based models in differential diagnosis. We combined the internal and external validation cohorts together and excluded healthy volunteers from them to create a differential diagnosis cohort for HCC and PDAC, respectively. The iPBIScore-based model showed an AUC value of 0.97 for HCC differentiation from other hepatic benign diseases, and an AUC value of 0.92 for PDAC differentiation from other pancreatic benign diseases (online supplemental figure S5). Thus, our strategy also had satisfying performance in scenario of differential diagnosis of hepatic and pancreatic lesions.

The performance of PBIScore-based models in early-stage and tumour-marker-negative tumours

Detection of early-stage tumours and those that are negative for tumour markers is more challenging in clinical practice. To test the role of our model in these scenarios, we first analysed the performance of models in different stages of HCC and PDAC. In general, the variations between cancers and non-cancers were more significant than the difference between stages for both HCC and PDAC, although in some cohorts, advanced tumours demonstrated a more obvious feature than early-stage tumours (online supplemental figure S6).

We then tested the PBIScore-based models in participants with HCC at stage 0 or A. Compared with an AUC of 0.81 for AFP, the PBIScore model and iPBIScore model demonstrated AUC values of 0.90 and 0.96, respectively (figure 5A). In participants with resectable PDAC, CA19-9 showed an AUC of 0.88; however, the PBIScore model and iPBIScore model achieved AUC values of 0.89 and 0.95, respectively (figure 5B). These results verified the good performance of the models to detect early-stage tumours.

AFP and CA19-9 are the most frequently used tumour markers for HCC and PDAC, respectively; therefore, patients who are negative for these tumour markers are easily overlooked. We collected all AFP-negative HCC and CA19-9-negative PDAC in the validation cohorts, and used them to test the performance of the PBIScore model. Our model showed an AUC of 0.91 in HCC and 0.86 in PDAC, respectively (figure 5C,D). Therefore, the

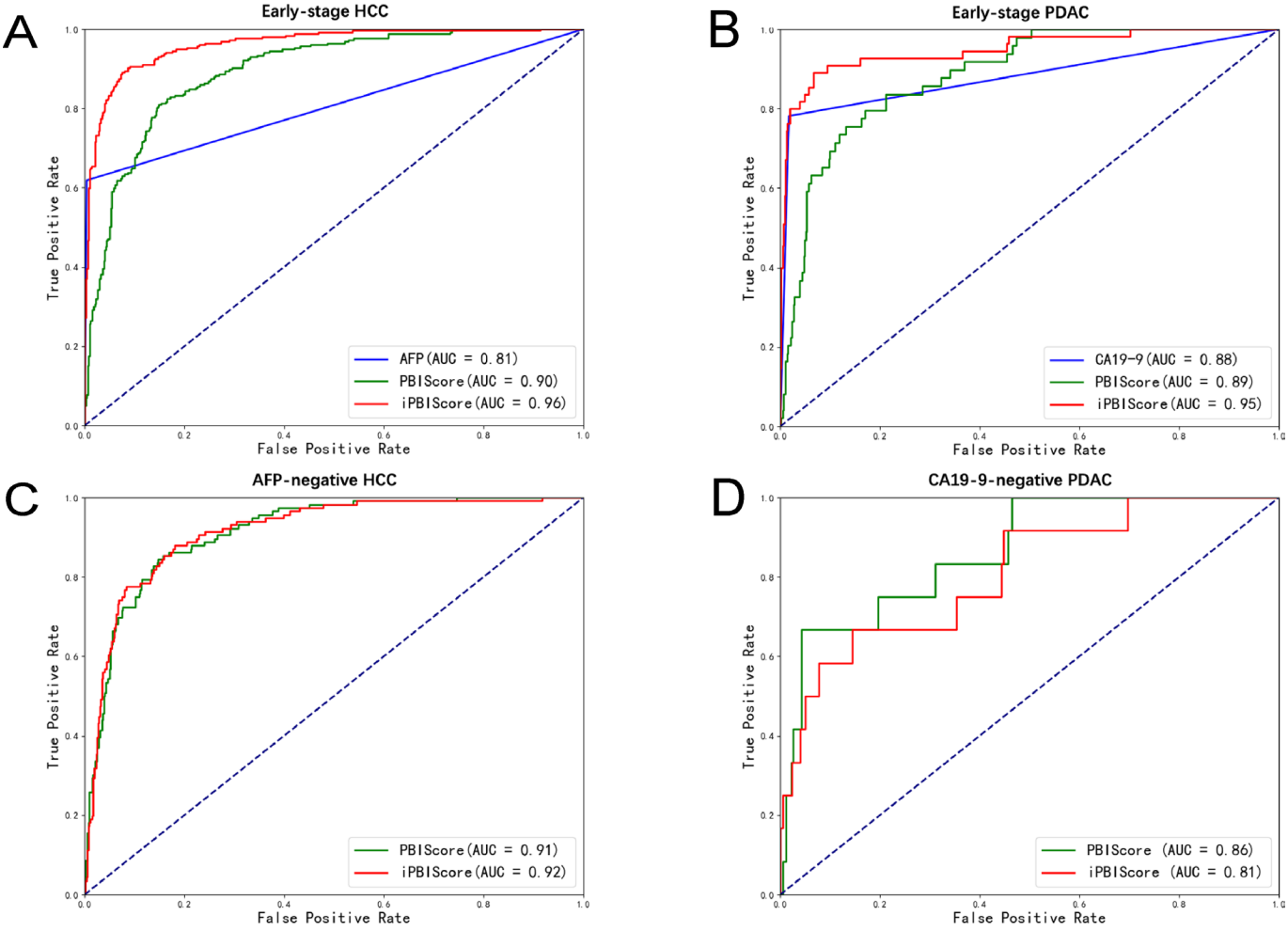

Figure 5 Performance of the tumour detection models in patients with early-stage disease or those with a normal level of tumour markers. (A) The ROC curves of AFP, PBIScore and iPBIScore for tumour detection in patients with HCC stage 0–A stage, showing an AUC of 0.81, 0.90 and 0.96, respectively. (B) The ROC curves of CA19-9, PBIScore and iPBIScore for tumour detection in patients with resectable pancreatic cancer, showing an AUC of 0.88, 0.89 and 0.95, respectively. (C) The ROC curves of PBIScore and iPBIScore for tumour detection in AFP-negative HCC, showing an AUC of 0.91 and 0.92, respectively. (D) The ROC curves of PBIScore and iPBIScore for tumour detection in CA19-9-negative PDAC, showing an AUC of 0.86 and 0.81, respectively. AFP, alpha-fetoprotein; AUC, area under the curve; CA19-9, carcinoma antigen 19-9; HCC, hepatocellular carcinoma iPBIScore, integrated peripheral blood immune score; PBIScore, peripheral blood immune score; PDAC, pancreatic ductal adenocarcinoma; ROC, receiver operating characteristic.

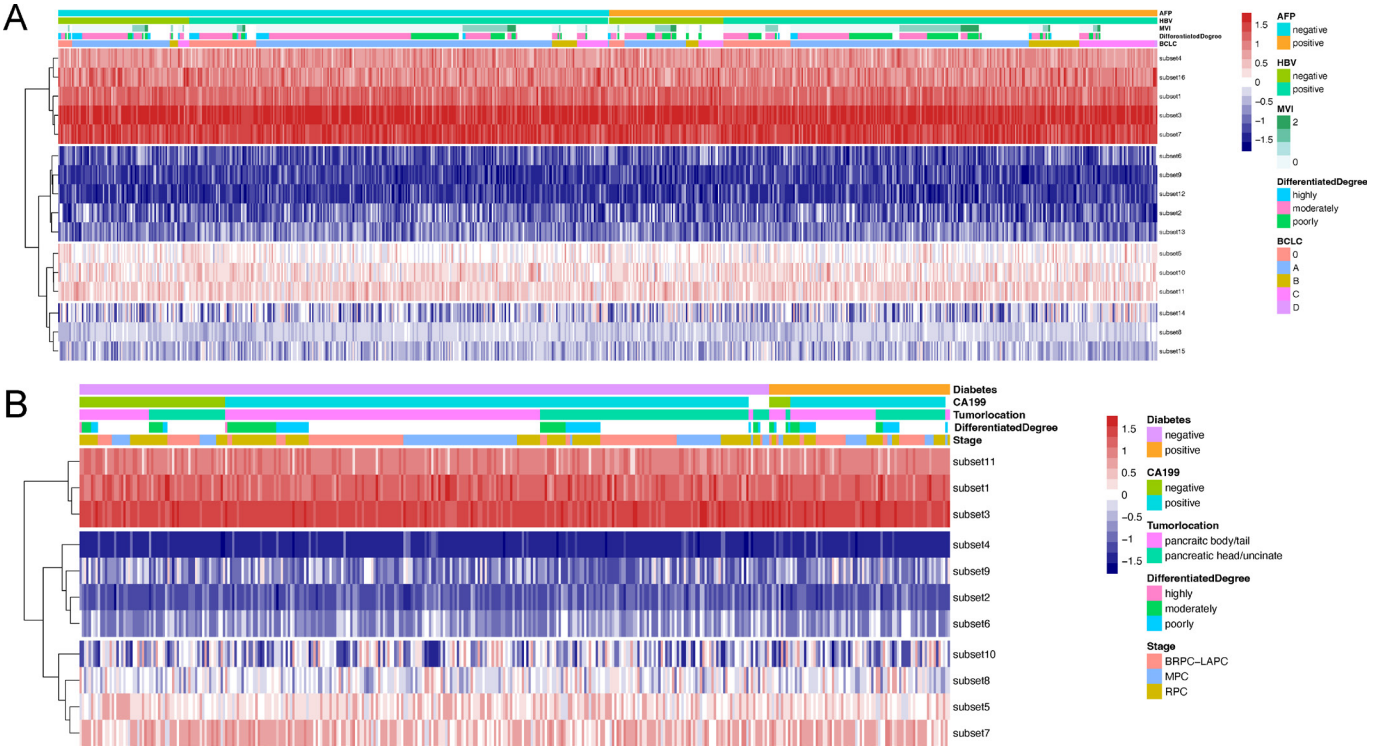

Figure 6 The relationship between the cell subsets used for model construction and the tumour features. (A) Heatmap depicting the relationship between the abundance of characteristic subgroups used to construct models and the various clinicopathological features of HCC. (B) Heatmap depicting the relationship between the abundance of characteristic subgroups used to construct the models and the various clinicopathological features of PDAC. AFP, alpha-fetoprotein; BCLC, Barcelona Clinic Liver Cancer; CA19-9, carcinoma antigen 19-9; HBV, Hepatitis B Virus; HCC, hepatocellular carcinoma; MVI, microvascular invasion; PDAC, pancreatic ductal adenocarcinoma.

PBIScore could be a good complement for traditional tumour markers.

Relationship between clinicopathological features and peripheral immune status

Given the satisfactory performance of the PBIScore-based models, we investigated the potential subtypes among the patients with tumours. Important clinicopathological parameters, such as tumour markers, tumour differentiation degree and disease stages were analysed. We re-clustered the cell subsets included in the PBIScore-based models, and compared their proportions across these clinicopathological parameters (figure 6). Among the 790 participants with HCC, the proportion of peripheral non-classical monocyte ($CD14^+CD16^+$) and central memory $CD8^+$ T cell ($CCR7^+CD45RA^-$) was significantly less in AFP-positive participants than in AFP-negative participants (online supplemental table S9). Notably, $CD3^-CD19^-CD14^+$ monocytes and $HLA\text{-}DR^+CD38^+CD8^+$ T cells were enriched whereas $CD33^-CD14^-$ lymphocytes decreased in patients with Hepatitis B Virus (HBV) infection. The proportion of central memory $CD8^+$ T cell was higher in patients with moderate or well-differentiated HCC than that in patients with poorly-differentiated HCC. Intriguingly, advanced HCC was associated with markedly higher proportions of seven cell subsets, including monocytes, $HLA\text{-}DR^+CD38^+CD8^+$ T cells, $CD85j^-CD8^+$ T cells, $CXCR5^+CD8^+$ T cells, central memory $CD8^+$ T cells, myeloid-derived suppressor cells (MDSCs, $CD33^+CD3^-CD19^-HLA\text{-}DR^-CD11b^+$) and $CD33^-CD14^-$ lymphocytes. No featured cell subsets were identified in patients with HCC with different microvascular invasion status.

Among the 376 participants with PDAC, we noticed that tumour location and disease stage was significantly associated with many key cell subsets included in our models (online supplemental table S10). Patients with PDAC located in the body or tail of the pancreas showed more $HLA\text{-}DR^+CD38^+CD8^+$ T cells and $HLA\text{-}DR^+CD38^+CD4^+$ T cells in their peripheral blood. In contrast to HCC, the differentiation degree of PDAC did not influence these immune subsets in circulation; however, advanced PDAC demonstrated a higher level of lymphocytes, $HLA\text{-}DR^+CD38^+CD4^+$ T cells, MDSCs and $CD3^-CD19^-CD14^+$ monocytes compared with those in early-stage PDAC. Our results determined the relevance of immune cell subsets between the primary tumour and peripheral immune status, and defined some cell subsets that might have important influence in peripheral immune imbalance.

DISCUSSION

The development, progression and metastasis of a tumour are all closely related to antitumour immunity.[34] While much is known about the local immunity of the tumour microenvironment,[35] there has been little exploration of the relationship between the tumour and systemic immunity. Theoretically, the battle between the tumour and body immunity is supposed to be reflected in the peripheral blood, which constantly communicates with the tumour. For example, when the haematopoietical function of the tumour-bearing host was damaged extensively, the immature neutrophils and monocytes in the peripheral blood expanded abnormally, with some of them being metastasised to the tumour microenvironment, leading to local immunosuppression.[32 33]

To the best of our knowledge, this is the largest study using CyTOF analysis on human peripheral blood to date and is the first multicentre report using CyTOF as a tool for tumour diagnosis. In the current study, we took advantage of the high-dimensional profiling ability of CyTOF to discover the differences in immune cells populations of peripheral blood and subsequently used selected parameters in this process to generate tumour detection models with relatively high sensitivity and specificity. The success of our strategy in early-stage HCC and PDAC suggested that hints of tumours in peripheral blood might exist soon after tumour initiation, which supports the concept of analysing systemic immunity for early tumour detection. In addition, we used the same panel and strategy for two types of tumour, and obtained relatively similar results, not only for the performance of detection models, but also in the cell subsets identified for model construction and for their underlying clinical relevance. Therefore, these findings implied that our PBIScore-based strategy is probably applicable to other tumours. Nevertheless, compared with other liquid biopsy strategies, like ctDNA and CTC, our approach has a low requirement for sample collection, with only a 5 mL sample and no need to isolate rare cells or enrich low-abundance nucleotides. Therefore, it is more customer-friendly and easier to generalise. However, some important issues need to be overcome before CyTOF technique can be translated to clinic. For instance, although CyTOF is highly sensitive, the possibility of contamination especially by heavy metals is high.[36] Although CyTOF was validated to be well equivalent to flow cytometry that has been clinically used, an optimal panel of CyTOF is critical.[37] The metals for antibody labelling should be carefully chosen according to the expression intensity of biomarkers to avoid signal 'spillover'.[37] The data analysis of CyTOF is challenging and are currently different in many groups. We have designed an automatic gating algorithm for our study. A uniform process including both sample and data managements is needed for clinical criteria. Moreover, the acquisition time is relatively long for CyTOF, limiting the number of samples that can be detected every day.

Our detection models have a high value of AUC, which suggested a good performance. Trade-off between the sensitivity and specificity is dependent on different clinical scenarios. Although the sensitivity was relatively low at a specificity of 99% as most diagnostic tools were, as a liquid biopsy method focusing on tumour screening, we believe both sensitivity and specificity of around 90% is acceptable. Even though the PBIScore itself is superior to AFP or CA19-9, their combination further improved the AUC value. Notably, the PBIScore and these traditional tumour markers are mutually complementary with each other, which led to the outstanding performance of the iPBIScore detection model. Tumour markers like AFP and CA19-9 are directly derived from tumour cells. However, the PBIScore reflects the interaction between the human body and the tumour, which provides another angle for tumour tracing. Concern about the value of such an interaction was raised, because it can be affected by many physiological and pathophysiological factors, such as circadian rhythm, and thus is unstable. Strikingly, our results demonstrated that this concern might be misplaced. At least the alteration of some key cell markers or subsets is stable enough to detect the tumour. Further in-depth researches are needed to understand why patients with negative tumour markers have more significant changes in their peripheral immune cells.

The present study also identified several key cell subsets that may be responsible for the efficacy of the models. Numbers of naïve $CD4^+$ T cells and naïve $CD8^+$ T cells decreased in the peripheral blood of tumour-bearing participants, which limited the source of antitumour T cells in the tumour microenvironment. The frequency of $CD39^+$ monocytes significantly increased in participants with HCC or PDAC (C27 and C28 in online supplemental figures S1 and S3). CD39, believed to be a metabolic checkpoint, is a rate-limiting enzyme involved in adenosine production, which plays an important immunosuppressive role in the tumour microenvironment.[38] Intriguingly, the frequency of HLA-$DR^+CD38^+CD8^+$ T cells significantly increased in participants with advanced HCC (online supplemental table S9), suggesting that this cell subset was a biomarker of tumour progression in the circulation. In fact, the expression of both HLA-DR and CD38 on $CD8^+$ T cells in peripheral blood was reported to be correlated with advanced tumours.[39] HLA-$DR^+CD38^+CD8^+$ T cells are activated phenotype and may play key roles in antitumour immunity in both tumour microenvironment and peripheral blood.[40 41] Besides, in patients with HCC and those with PDAC, the proportion of monocytes increased gradually as the disease stage advanced, which was in line with previous studies showing that a high level of peripheral monocytes was found in such patients and was associated with their poor prognosis.[42–44] Overall, these findings broadened our understanding of the underlying reasons that peripheral blood could reflect tumour existence. However, the associations between model-related key cell subsets and clinicopathological parameters of patients were only statistical based and far away from scientific causality.

There are some limitations to our research. First, all participants came from China and were not internationally representative; however, we believe that the current method can be implemented in different ethnic groups and regions worldwide, given the nature of our strategy, though the parameters of the models will be modified to some extent. Second, people with haematological system diseases and those with recent bleeding or blood transfusion were excluded from the study, which limits the targeted population of our model. Third, we only developed tumour-type-specific models for HCC and PDAC, and whether the strategy can be used for pan-cancer screening is unknown. Fourth, our validation cohorts contained a high proportion of participants with malignant diseases, which was not the case for tumour detection in the real world. A natural population-based or high-risk population-based cohort study is needed for further evaluation of our models in clinical practice. The deficiency of patients with hepatitis or cirrhosis in our non-HCC cohort did not allow us to verify the efficacy of our models in these populations, which was another drawback, as more attention would have paid in the high-risk group. Additionally, our analyses of AFP and CA19-9 were based on a discrete way rather than using continuous variables due to unavailability of accurate values within the normal range in some healthy participants. Using them as continuous variables is likely to identify the best threshold to maximise sensitivity and specificity of the models. However, dealing with them as discrete variables also have advantages, for example, it will not change the current clinical practice too much and will be easier to be accepted by physicians. Last but not least, the age and gender were not always balanced in different groups, which could introduce biases and affect the performance of our model in certain cohorts. However, malignant tumours and benign diseases naturally have distinct age and gender tendencies. Age-related or gender-related alterations of immune cells are also features of tumour, no matter they are caused by the tumour or just companied with it. The purpose of our study was to develop an efficient tool to diagnose cancer, and our multicentre external validation confirmed the performance of our models.

In conclusion, we verified the differences in systemic immunity in patients with solid tumours, and used large-volume, multi-centre cohorts to demonstrate that PBIScore-based models show high performance for tumour detection. Therefore, we provide a ready-to-use tool for HCC and PDAC screening as an expansion of liquid biopsy. Our strategy also lays the foundation for future systemic immunity-based detection methods for pan-cancers.

Author affiliations
[1]Department of Hepatobiliary and Pancreatic Surgery, The First Affiliated Hospital, Zhejiang University School of Medicine, Hangzhou, China
[2]Zhejiang Provincial Key Laboratory of Pancreatic Disease, The First Affiliated Hospital, Zhejiang University School of Medicine, Hangzhou, China
[3]Zhejiang Clinical Research Center of Hepatobiliary and Pancreatic Diseases, Hangzhou, China
[4]The Innovation Center for the Study of Pancreatic Diseases of Zhejiang Province, Hangzhou, China
[5]Cancer Center, Zhejiang University, Hangzhou, China
[6]Alibaba Zhejiang University Joint Research Center of Future Digital Healthcare, Hangzhou, China
[7]Zhejiang Puluoting Health Technology Co Ltd, Hangzhou, China
[8]Department of Hepatobiliary and Pancreatic Surgery and Minimally Invasive Surgery, Zhejiang Provincial People's Hospital, Affiliated People's Hospital, Hangzhou Medical College, Hangzhou, China
[9]Department of Hepatobiliary and Pancreatic Surgery, The First Affiliated Hospital, Wenzhou University School of Medicine, Wenzhou, China
[10]Department of Hepatobiliary and Pancreatic Surgery, The Cancer Hospital of the University of Chinese Academy of Sciences (Zhejiang Cancer Hospital), Institute of Basic Medicine and Cancer, Chinese Academy of Sciences, Hangzhou, China
[11]Department of Medical Oncology, Sanmen People's Hospital, Taizhou, China
[12]Department of General Surgery, Huzhou Central Hospital, Zhejiang University School of Medicine, Huzhou, China
[13]Department of Surgery, Changxing People's Hospital, Huzhou, China
[14]Department of General Surgery, Ningbo Medical Center Lihuili Eastern Hospital, Ningbo, China
[15]Department of General Surgery, Shengzhou People's Hospital, Shengzhou, China
[16]Department of General Surgery, Haining People's Hospital, Haining, China
[17]Department of General Surgery, Jiaxing Second People's Hospital, Jiaxing, China
[18]Department of Hepatobiliary and Pancreatic Surgery, The Second Affiliated Hospital of Nanchang University, Nanchang, China
[19]Department of General Surgery, Shangyu People's Hospital of Shaoxing, Shangyu, China
[20]Department of Hepatobiliary and Pancreatic Surgery, The Second Hospital of Hebei Medical University, Shijiazhuang, China
[21]Department of General Surgery, Jixi County People's Hospital, Jixi, China
[22]Department of Gastroenterology, The First Affiliated Hospital, Zhejiang University School of Medicine, Hangzhou, China

Correction notice This article has been corrected since it published Online First. The author names, Mao Ye and Tianxing Yang, have been updated.

Acknowledgements We sincerely appreciate colleagues of the hospitals participating in this study for their help of sample collection and discussion. We thank Dr Jie Wu from State Key Laboratory for Diagnosis and Treatment of Infectious Diseases of China for his technical support of statistics.

Contributors TL and QZ conceived the idea and designed the study. TL supervised the whole study. QZ, YM, MH, YW, YL, JZ, JL, YZ, TY, XS, WY, YH, HH, MX, XW, XY, WT, RL, YG, TW, JW, XW and JW collected the samples. CL and TW provided metal-conjugated antibodies and conducted sample processing. QZ, YM, CL, QK and TW analysed the data. TL, QZ, XB, CY, CZ and ZY interpreted the results. QZ and YM drafted the manuscript. All authors made revision and approved the final version of manuscript. TL is the guarantor.

Funding This work was financially supported by the National Key Research and Development Program of China (Nos. 2020YFA0804300/2020YFA0804301, 2019YFC1315800/2019YFC1315802), National Natural Science Foundation of China (Nos. 82188102, U20A20378), the Key Research & Development Program of Zhejiang Province (Nos. 2021C03063, 2019C03019), Zhejiang Provincial Natural Science Foundation of China (No. LR20H160002), the Joint Funds of the Zhejiang Provincial Natural Science Foundation of China (No. HDMD22H319373), the Key Research Project of Zhejiang Lab (No. 2022ND0AC01). This work also was supported by Alibaba Cloud.

Competing interests None declared.

Patient and public involvement Patients and/or the public were not involved in the design, or conduct, or reporting, or dissemination plans of this research.

Patient consent for publication Not applicable.

Ethics approval The human research ethics committees at the First Affiliated Hospital, Zhejiang University School of Medicine, Hangzhou, China (2019-1445-1, 2020-835); Zhejiang Provincial People's Hospital, Affiliated People's Hospital, Hangzhou Medical College, Hangzhou, Zhejiang, China (2021KY027); The First Affiliated Hospital, Wenzhou University School of Medicine, Wenzhou, China (2021-075); The Cancer Hospital of the University of Chinese Academy of Sciences (Zhejiang Cancer Hospital), Institute of Basic Medicine and Cancer, Chinese Academy of Sciences, Hangzhou, China (IRB-2021-206); Sanmen People's Hospital, Taizhou, China (2020-121); Huzhou Central Hospital, Zhejiang University School of Medicine, Huzhou, China (2021206-01); Changxing People's Hospital, Huzhou, China (2020-057); Ningbo Medical Center Lihuili Eastern Hospital, Ningbo, China (KY2020SL178); Shengzhou People's Hospital, Shengzhou, China (2022-001); Haining People's Hospital, Haining, China (2021-11); Jiaxing Second People's Hospital, Jiaxing, China (JXEY-WYZF009); The Second Affiliated Hospital of Nanchang University, Nanchang, China (waived, accepting ethics approval of the leading institute); Shangyu Hospital of Chinese Medicine, Shaoxing, China (2021-02-06); The Second Hospital of Hebei Medical University, Shijiazhuang, China (2021-R135); Jixi County People's Hospital, Xuancheng, China (2021-01). Informed consent was obtained from all participants before collecting peripheral blood samples.

Provenance and peer review Not commissioned; externally peer reviewed.

Data availability statement Data are available upon reasonable request.

ORCID iDs
Qi Zhang http://orcid.org/0000-0002-6096-0690
Chaohui Yu http://orcid.org/0000-0003-4842-3646
Xueli Bai http://orcid.org/0000-0002-2934-0880

REFERENCES

1 Gupta S, Bent S, Kohlwes J. Test characteristics of alpha-fetoprotein for detecting hepatocellular carcinoma in patients with hepatitis C. a systematic review and critical analysis. *Ann Intern Med* 2003;139:46–50.
2 Melbye M, Wohlfahrt J, Lei U, *et al*. Alpha-Fetoprotein levels in maternal serum during pregnancy and maternal breast cancer incidence. *J Natl Cancer Inst* 2000;92:1001–5.
3 Di Bisceglie AM, Sterling RK, Chung RT, *et al*. Serum alpha-fetoprotein levels in patients with advanced hepatitis C: results from the HALT-C trial. *J Hepatol* 2005;43:434–41.
4 Ballehaninna UK, Chamberlain RS. The clinical utility of serum Ca 19-9 in the diagnosis, prognosis and management of pancreatic adenocarcinoma: an evidence based appraisal. *J Gastrointest Oncol* 2012;3:105–19.
5 Greca GL*et al*. Adjusting CA19-9 values to predict malignancy in obstructive jaundice: influence of bilirubin and C-reactive protein. *World J Gastroenterol* 2012;18:4150–5.
6 Hogendorf P, Skulimowski A, Durczyński A, *et al*. A panel of CA19-9, CA125, and CA15-3 as the enhanced test for the differential diagnosis of the pancreatic lesion. *Dis Markers* 2017;2017:8629712
7 Su S-B, Qin S-Y, Chen W, *et al*. Carbohydrate antigen 19-9 for differential diagnosis of pancreatic carcinoma and chronic pancreatitis. *World J Gastroenterol* 2015;21:4323–33.
8 Ignatiadis M, Sledge GW, Jeffrey SS. Liquid biopsy enters the clinic — implementation issues and future challenges. *Nat Rev Clin Oncol* 2021;18:297–312.
9 Luo P, Yin P, Hua R, *et al*. A Large-scale, multicenter serum metabolite biomarker identification study for the early detection of hepatocellular carcinoma. *Hepatology* 2018;67:662–75.
10 Cai J, Chen L, Zhang Z, *et al*. Genome-Wide mapping of 5-hydroxymethylcytosines in circulating cell-free DNA as a non-invasive approach for early detection of hepatocellular carcinoma. *Gut* 2019;68:2195–205.
11 Xu R-H, Wei W, Krawczyk M, *et al*. Circulating tumour DNA methylation markers for diagnosis and prognosis of hepatocellular carcinoma. *Nat Mater* 2017;16:1155–61.
12 Conforti F, Pala L, Bagnardi V, *et al*. Cancer immunotherapy efficacy and patients' sex: a systematic review and meta-analysis. *Lancet Oncol* 2018;19:737–46.

13 Finn RS, Qin S, Ikeda M, *et al*. Atezolizumab plus bevacizumab in unresectable hepatocellular carcinoma. *N Engl J Med Overseas Ed* 2020;382:1894–905.
14 Socinski MA, Jotte RM, Cappuzzo F, *et al*. Atezolizumab for first-line treatment of metastatic nonsquamous NSCLC. *N Engl J Med Overseas Ed* 2018;378:2288–301.
15 Allen BM, Hiam KJ, Burnett CE, *et al*. Systemic dysfunction and plasticity of the immune macroenvironment in cancer models. *Nat Med* 2020;26:1125–34.
16 Schultze JL, Mass E, Schlitzer A. Emerging principles in myelopoiesis at homeostasis and during infection and inflammation. *Immunity* 2019;50:288–301.
17 Masopust D, Schenkel JM. The integration of T cell migration, differentiation and function. *Nat Rev Immunol* 2013;13:309–20.
18 Wang L, Simons DL, Lu X, *et al*. Connecting blood and intratumoral Treg cell activity in predicting future relapse in breast cancer. *Nat Immunol* 2019;20:1220–30.
19 Murakami Y, Saito H, Shimizu S, *et al*. Increased regulatory B cells are involved in immune evasion in patients with gastric cancer. *Sci Rep* 2019;9:13083.
20 Zhou J, Min Z, Zhang D, *et al*. Enhanced frequency and potential mechanism of B regulatory cells in patients with lung cancer. *J Transl Med* 2014;12:304.
21 Mamessier E, Sylvain A, Thibult M-L, *et al*. Human breast cancer cells enhance self tolerance by promoting evasion from NK cell antitumor immunity. *J Clin Invest* 2011;121:3609–22.
22 WC W, Sun HW, Chen HT. Circulating hematopoietic stem and progenitor cells are myeloid-biased in cancer patients. *Proc Natl Acad Sci U S A* 2014;111:4221–6.
23 Templeton AJ, McNamara MG, Šeruga B, *et al*. Prognostic role of neutrophil-to-lymphocyte ratio in solid tumors: a systematic review and meta-analysis. *J Natl Cancer Inst* 2014;106:dju124.
24 van Cruijsen H, van der Veldt AAM, Vroling L, *et al*. Sunitinib-Induced myeloid lineage redistribution in renal cell cancer patients: CD1c+ dendritic cell frequency predicts progression-free survival. *Clin Cancer Res* 2008;14:5884–92.
25 Finotello F, Rieder D, Hackl H, *et al*. Next-Generation computational tools for interrogating cancer immunity. *Nat Rev Genet* 2019;20:724–46.
26 Simoni Y, Fehlings M, Kløverpris HN, *et al*. Human innate lymphoid cell subsets possess tissue-type based heterogeneity in phenotype and frequency. *Immunity* 2017;46:148–61.
27 Levine LS, Hiam-Galvez KJ, Marquez DM, *et al*. Single-cell analysis by mass cytometry reveals metabolic states of early-activated CD8+ T cells during the primary immune response. *Immunity* 2021;54:829–44.
28 Zunder ER, Finck R, Behbehani GK, *et al*. Palladium-based mass tag cell barcoding with a doublet-filtering scheme and single-cell deconvolution algorithm. *Nat Protoc* 2015;10:316–33.
29 Finck R, Simonds EF, Jager A, *et al*. Normalization of mass cytometry data with bead standards. *Cytometry* 2013;83A:483–94.
30 Samusik N, Good Z, Spitzer MH, *et al*. Automated mapping of phenotype space with single-cell data. *Nat Methods* 2016;13:493–6.
31 Laurens VDM, Hinton G. Visualizing data using t-SNE. *J Mach Learn Res* 2008;9:2579–605.
32 Gabrilovich DI, Ostrand-Rosenberg S, Bronte V. Coordinated regulation of myeloid cells by tumours. *Nat Rev Immunol* 2012;12:253–68.
33 Jaillon S, Ponzetta A, Di Mitri D, *et al*. Neutrophil diversity and plasticity in tumour progression and therapy. *Nat Rev Cancer* 2020;20:485–503.
34 Galon J, Pagès F, Marincola FM, *et al*. The immune score as a new possible approach for the classification of cancer. *J Transl Med* 2012;10:1.
35 Fridman WH, Zitvogel L, Sautès-Fridman C, *et al*. The immune contexture in cancer prognosis and treatment. *Nat Rev Clin Oncol* 2017;14:717–34.
36 Spitzer MH, Nolan GP. Mass cytometry: single cells, many features. *Cell* 2016;165:780–91.
37 Gadalla R, Noamani B, MacLeod BL, *et al*. Validation of CyTOF against flow cytometry for immunological studies and monitoring of human cancer clinical trials. *Front Oncol* 2019;9:415.
38 Perrot I, Michaud H-A, Giraudon-Paoli M, *et al*. Blocking antibodies targeting the CD39/CD73 immunosuppressive pathway Unleash immune responses in combination cancer therapies. *Cell Rep* 2019;27:2411–25.
39 Wang Y-Y, Zhou N, Liu H-S, *et al*. Circulating activated lymphocyte subsets as potential blood biomarkers of cancer progression. *Cancer Med* 2020;9:5086–94.
40 de Vries NL, van Unen V, Ijsselsteijn ME, *et al*. High-dimensional cytometric analysis of colorectal cancer reveals novel mediators of antitumour immunity. *Gut* 2020;69:691–703.
41 Kamphorst AO, Pillai RN, Yang S, *et al*. Proliferation of PD-1+ CD8 T cells in peripheral blood after PD-1–targeted therapy in lung cancer patients. *Proc Natl Acad Sci U S A* 2017;114:4993–8.
42 Juusola M, Kuuliala K, Kuuliala A, *et al*. Pancreatic cancer is associated with aberrant monocyte function and successive differentiation into macrophages with inferior anti-tumour characteristics. *Pancreatology* 2021;21:397–405.
43 Shen S-L, Fu S-J, Huang X-Q, *et al*. Elevated preoperative peripheral blood monocyte count predicts poor prognosis for hepatocellular carcinoma after curative resection. *BMC Cancer* 2014;14:744.
44 Kubota K, Shimizu A, Notake T, *et al*. Preoperative peripheral blood lymphocyte-to-monocyte ratio predicts long-term outcome for patients with pancreatic ductal adenocarcinoma. *Ann Surg Oncol* 2022;29:1437–48.